Heliyon

ELSEVIER

Received:
24 September 2018
Revised:
21 December 2018
Accepted:
22 January 2019

Cite as: J. Melo Quintero, K.L. Salcedo Rodríguez, F.A. Gómez Albarracín, H.D. Rosales, P. Mendoza Zélis, S.J. Stewart, L.A. Errico, C. Rodríguez Torres. On the deviation from a Curie–Weiss behavior of the $ZnFe_2O_4$ susceptibility: A combined ab-initio and Monte-Carlo approach. Heliyon 5 (2019) e01170. doi: 10.1016/j.heliyon.2019.e01170

On the deviation from a Curie–Weiss behavior of the $ZnFe_2O_4$ susceptibility: A combined ab-initio and Monte-Carlo approach

J. Melo Quintero [a], **K.L. Salcedo Rodríguez** [a], **F.A. Gómez Albarracín** [b], **H.D. Rosales** [b,c], **P. Mendoza Zélis** [a], **S.J. Stewart** [a], **L.A. Errico** [a], **C. Rodríguez Torres** [a,*]

[a] *Instituto de Física La Plata, CCT La Plata, CONICET and Departamento de Física, Facultad de Ciencias Exactas, Universidad Nacional de La Plata, C.C. 67, 1900 La Plata, Argentina*

[b] *Instituto de Física de Líquidos y Sistemas Biológicos, CCT La Plata, CONICET and Departamento de Física, Facultad de Ciencias Exactas, Universidad Nacional de La Plata, C.C. 67, 1900 La Plata, Argentina*

[c] *Facultad de Ingeniería, Universidad Nacional de La Plata, 1900 La Plata, Argentina*

* Corresponding author.
E-mail address: torres@fisica.unlp.edu.ar (C. Rodríguez Torres).

Abstract

We present a numerical study of the magnetic properties of $ZnFe_2O_4$ using Monte-Carlo simulations performed considering a Heisenberg model with antiferromagnetic couplings determined by Density Functional Theory. Our calculations predict that the magnetic susceptibility has a cusp-like peak centered at 13 K, and follows a Curie–Weiss behavior above this temperature with a high and negative Curie–Weiss temperature ($\Theta_{CW} = -170$ K). These results agree with the experimental data once extrinsic contributions that give rise to the deviation from a Curie–Weiss law are discounted. Additionally, we discuss the spin configuration of $ZnFe_2O_4$ below its ordering temperature, where the system presents a high degeneracy.

Keywords: Condensed matter physics

https://doi.org/10.1016/j.heliyon.2019.e01170

1. Introduction

The underlying magnetism of the spinel ferrite $ZnFe_2O_4$ has been of interest over the last three decades in the condensed matter community [1, 2, 3, 4, 5]. $ZnFe_2O_4$ in its normal structure (i.e., with Fe^{3+} and Zn^{2+} ions at octahedral B and tetrahedral A-sites, respectively) is widely identified as an antiferromagnet insulator with a Néel temperature (T_N) around 10 K and a band gap of 0.2 eV [1, 6]. However, its low temperature magnetic state has been the subject of discussion leading to different proposals [1, 3, 4, 7]. The B-sites in spinel compounds form a network of corner-sharing tetrahedra known as the pyrochlore lattice. This type of network, also characteristic of $A_2B_2O_7$ compounds, is susceptible to geometrical frustration when the spin are coupled antiferromagnetically [8, 9]. The macroscopic degeneracy of the ground state of geometrically frustrated compounds can give rise to glassy magnetic behaviors and even lead to the inhibition of a long-range order (LRO) [8, 9, 10, 11, 12]. In fact, the LRO detected in nominally normal $ZnFe_2O_4$ [4] has been attributed to the presence of extrinsic defects [3]. Indeed, neutron scattering results on high-purity $ZnFe_2O_4$ single-crystal indicated that the compound remains magnetically disordered (at least partially) even at temperatures as low as 1.5 K [1].

Concerning the macroscopic magnetic properties, the susceptibility (χ) of $ZnFe_2O_4$ is characterized by a well-defined cusp-like peak centered at around 11–13 K, i.e. nearby the reported T_N [1, 3]. Further, the reciprocal susceptibility (χ^{-1}) deviates from a Curie–Weiss (C-W) behavior below 280 K [1]. The extrapolated Curie–Weiss temperature (Θ_{CW}), which is related to the strength and type of magnetic interactions, it has been reported to be positive with values as high as +120 K [1]. The fact that the absolute value of Θ_{CW} is one order of magnitude larger than T_N has been taken as an empiric evidence that $ZnFe_2O_4$ belongs to the group of strongly geometrically frustrated compounds [9, 10]. However, instead of the negative Θ_{CW} found for isomorphic spinels with strong geometric frustration, such as $ZnCr_2O_4$ and $CdFe_2O_4$ [9, 13, 14], the positive Θ_{CW} usually reported for $ZnFe_2O_4$ [3] would suggest the existence of ferromagnetic (FM) instead of antiferromagnetic (AFM) nearest-neighbors interactions predicted for these normal spinels. In theory, this description would contradict the classification of $ZnFe_2O_4$ as a geometrically frustrated compound [9, 10]. Kamazawa et al. [1] attributed the unusual behavior of $ZnFe_2O_4$ to the frustration arising from the competition between AFM coupled third-neighbor interactions (J_3) and the first-neighbor interactions (J_1) that changes from FM to AFM type as the temperature decreases. This singular trend has been attributed to a thermal variation of the Fe^{3+}-O-Fe^{3+} bond angle, although this has not been detected experimentally [1, 15]. The influence of further neighbor exchange in pyrochlore compounds has been pointed out to be crucial for these systems to select between their multiple low temperature spin states [9, 16, 17]. Particularly, for $CdFe_2O_4$ and $ZnFe_2O_4$, Cheng [18] found that all interactions up to third-neighbor

 https://doi.org/10.1016/j.heliyon.2019.e01170

are AFM, being J_3 of the same order of magnitude as J_1. The different proposals for the magnetic moment interactions suggest that further investigation are needed to interpret the unusual magnetic features of $ZnFe_2O_4$, which make this compound to be one of the most intriguing among the set of frustrated spinels.

In this work we focus on the study of the magnetic susceptibility of $ZnFe_2O_4$ by combining ab-initio and Monte-Carlo calculations that are contrasted to experimental results. The paper is organized as follows. Considering as a first approach a normal $ZnFe_2O_4$ structure, in Sec. 2, we perform density functional theory (DFT)-based ab initio calculations to determine the energy of different spin configurations. These configurations are mapped into a Heisenberg spin model in order to obtain the magnetic exchange couplings. Then, we use these coupling to perform simulations with the Monte-Carlo Metropolis algorithm to obtain the susceptibility and heat capacity as function of temperature. In Sec. 3 we compare simulations with our previous experimental data and comment on the simulation results for lower temperatures, where the model presents a high degeneracy. Conclusions and future work are presented in Sec. 4.

2. Calculation

2.1. Ab-initio calculations

In order to obtain the exchange couplings we performed DFT-based first principles calculations. Firstly, we calculated the total energy of the different spin configurations assumed for $ZnFe_2O_4$. Subsequently, these configurations were mapped to an appropriate spin model to obtain the exchange couplings. Here we propose a Heisenberg spin Hamiltonian, given by:

$$H = -\sum_{n=1}^{N}\sum_{i'>i}^{l} J_n \vec{S}_i \cdot \vec{S}_{i'} \tag{1}$$

where $\vec{S}_i$ and $\vec{S}_{i'}$ are three dimensional unit vectors, and J_n are the exchange couplings. In spinel oxides the magnetic coupling is governed by superexchange couplings along $A-O-A$, $B-O-B$ and $A-O-B$ paths. In normal $ZnFe_2O_4$, the Fe^{3+} magnetic ions are located solely at B sites arranged in a pyrochlore-type lattice (Figure 1). Since Zn^{2+} ions are not polarized, only interactions through B sites will be present (i.e., $J_{BB} \neq 0$ and $J_{AB} = J_{AA} = 0$). Previous calculations performed by Cheng [18] revealed that the third-nearest neighbor interaction is of the same order of magnitude as first-nearest neighbor one. The J_3 interaction involves iron ions at a separation distance of 6.0 Å, which represents a long-ranged coupling. Hence, in order to ensure the convergence of the series of Eq. (1), we have considered the spin interactions up to fifth-neighbors (i.e., iron ions at 8.0 Å apart, $N = 5$ in Eq. (1)).

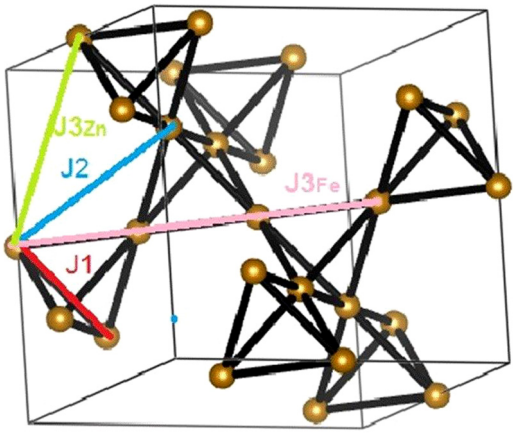

Figure 1. Pyrochlore lattice. First (J_1), second (J_2) and third-nearest neighbors (J_{3Fe} and J_{3Zn} for $ZnFe_2O_4$) are indicated.

Table 1. Number of coordination shell n, Fe–Fe$_n$ distances, and couplings J_n obtained from ab-initio calculations.

N_n	Number of spins	d (Å)	J_n (meV)
1	6	3.01	-2.8_1
2	12	5.22	-0.4_1
3	12	6.02	-1.3_1
4	12	6.70	-0.2_1
5	24	8.00	-0.06_{10}

Then, to build-up the equations derived from the Heisenberg model we take into account that each B-site has 6 B-sites as first-nearest neighbors (along one edge of a tetrahedron), 12 B-sites second-nearest neighbors (two non-collinear edges of two adjacent tetrahedrons), and 12 B-sites third-nearest neighbors (six along the first-nearest neighbor bonds and six across the hexagons in the kagome planes, denoted as J_{3Fe} and J_{3Zn} in Figure 1, respectively). Here we have considered an effective J_3. In the fourth and fifth coordination spheres there are 12 and 24 B-sites nearest-neighbors, respectively (see Table 1).

In order to obtain the J_n values ($n = 1 - 5$), five spin arrangements (plus the ferromagnetic one) are required. In the present work, to obtain accurate J_n values with their corresponding uncertainties, the energy of eleven independent magnetic configurations (one ferromagnetic, two ferrimagnetic and eight antiferromagnetic, see Table 2) were calculated and the J_n were then obtained through a least-square method. The calculations were performed using the WIEN2k code [19], an implementation of the full-potential linearized augmented plane waves plus local orbitals (FPLAPW+lo) method [20, 21]. In order to calculate the spin configurations a supercell (SC) with dimensions $\{a\times a\times 2a\}$ that contains 112 atoms (32 Fe, $l = 32$ in Eq. (1) was constructed from the 14-atoms primitive cell. With this SC size it is possible to obtain the independent magnetic configurations necessary to calculate

 https://doi.org/10.1016/j.heliyon.2019.e01170

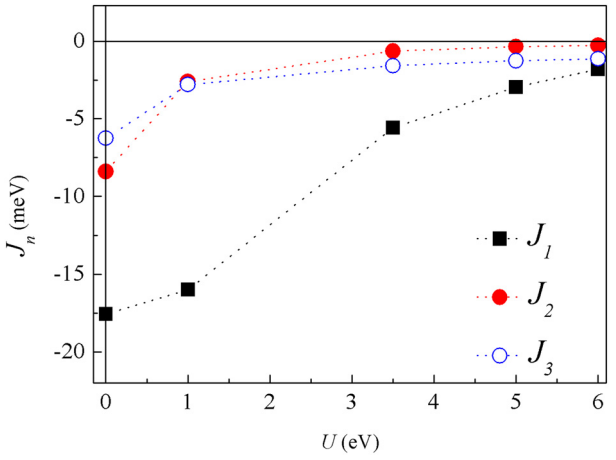

Figure 2. Exchange couplings J_n obtained from ab initio calculations considering interactions up to fifth neighbors as a function of the Hubbard U parameter. For simplicity, J_4 and J_5 were not included.

up to fifth neighbors exchange constant. The parameter RK_{MAX}, which controls the size of the basis set, was set to 7.0 (R is the smallest muffin tin radius and RK_{MAX} the largest wave number of the basis set). Integration in the reciprocal space was performed using the tetrahedron method taking 50 k-points in the first Brillouin zone. The muffin tin radius was chosen 1.06 Å for Zn and Fe, and 0.8 Å for O. Exchange and correlation effects were treated using the generalized gradient approximation (GGA [22])) plus an external Hubbard U term in the self-interaction-corrected scheme [23]. The results for the J_n exchange couplings as a function of the U values are shown in Figure 2. As can be seen, independently of the U values they are all negative (AFM). Further, our results indicate that an U increment produces a reduction in the J_n magnitudes. This behavior, which is consistent with those obtained in Ref. [18], is the expected one. Indeed, the effect of U on the electronic structure of $ZnFe_2O_4$ is to localize the d electrons of the Fe ions reducing hybridization and therefore weakening the interactions between them.

After studying a set of iron oxides as a function of U in the 0 to 6.0 eV range, a value $U = 5$ eV was selected based on the fact that this value reproduces the structural, electronic, magnetic and hyperfine parameters reported for these Fe-oxides and pristine $ZnFe_2O_4$ (see Ref. [24]). By examining the effect of different basis sets and k-point samplings we conclude that for $RK_{MAX} = 7$ and 50 k-points numerical errors are negligible and our results are very well converged (for a detailed description of our convergence tests, see Ref. [24]). In particular, the convergence degree achieved in the energy differences and the use of eleven spin configurations enable us to determine the J_n values with an accuracy of less than 0.1 meV. The uncertainties assigned to J values result from the least-square fitting using calculated energies and the following expressions:

$$\Delta E_{AF1} = -0.473 = 128J^1_{BB} + 256J^2_{BB} + 256J^4_{BB} + 512J^5_{BB}$$

$$\Delta E_{AF2} = -0.749 = 128J^1_{BB} + 128J^2_{BB} + 256J^3_{BB} + 256J^4_{BB} + 256J^5_{BB}$$
$$\Delta E_{AF3} = -0.646 = 96J^1_{BB} + 208J^2_{BB} + 224J^3_{BB} + 192J^4_{BB} + 416J^5_{BB}$$
$$\Delta E_{AF4} = -0.621 = 88J^1_{BB} + 224J^2_{BB} + 224J^3_{BB} + 176J^4_{BB} + 448J^5_{BB}$$
$$\Delta E_{AF5} = -0.702 = 120J^1_{BB} + 160J^2_{BB} + 224J^3_{BB} + 240J^4_{BB} + 320J^5_{BB}$$
$$\Delta E_{AF6} = -0.336 = 32J^1_{BB} + 128J^2_{BB} + 128J^3_{BB} + 128J^4_{BB} + 384J^5_{BB}$$
$$\Delta E_{AF7} = -0.632 = 120J^1_{BB} + 192J^2_{BB} + 160J^3_{BB} + 240J^4_{BB} + 384J^5_{BB}$$
$$\Delta E_{AF8} = -0.441 = 64J^1_{BB} + 192J^2_{BB} + 128J^3_{BB} + 160J^4_{BB} + 448J^5_{BB}$$
$$\Delta E_{FERRI1} = -0.098 = 12J^1_{BB} + 24J^2_{BB} + 24J^3_{BB} + 24J^4_{BB} + 48J^5_{BB}$$
$$\Delta E_{FERRI2} = -0.719 = 120J^1_{BB} + 144J^2_{BB} + 240J^3_{BB} + 240J^4_{BB} + 288J^5_{BB}$$

where energies E are in eV and equations are referred to the ferromagnetic case.

For each spin configuration, we obtained the equilibrium lattice parameters and all atoms in the SCs were allowed to completely relax to new equilibrium positions. For $U = 5$ eV, the lattice parameter a values and the magnetic moment of the Fe ions (μ_{Fe}) are in excellent agreement with experimental results ($a = 8.46$ Å for the eight antiferromagnetic spin arrangements, $a = 8.45$ Å for the ferri- and ferromagnetic cases, and $\mu_{\mathrm{Fe}} = 4.20\,\mu_B$ for all cases). It is worth mentioning that magnetic moments at the Fe sites are localized in the Fe-atomic spheres (a necessary condition for the application of the Heisenberg model) and $\mu_{\mathrm{Zn}} = 0$.

The resulting J_n values for $U = 5$ eV (those that will be used in the M-C simulations) are shown in Table 1. As can be seen, J_3 is of the same order of magnitude than J_1, being J_2 significantly smaller than J_3. A remarkable result is that J_4 and J_5 present small values. Therefore, it is a good approximation to consider the sum of Eq. (1) up to the third term.

Finally, to check the consistency of the method, we compare in Figure 3 the energy values (relative to the ferromagnetic case) of each proposed configuration determined using the obtained J_1, J_2 and J_3 couplings with those obtained through DFT calculations. The good agreement indicates that interactions up to third neighbors are adequate for the description of the magnetic interactions in $ZnFe_2O_4$.

2.2. Monte-Carlo simulations

In order to reproduce the susceptibility as a function of temperature we use the couplings constants obtained from ab-initio calculations as input data in Monte-Carlo (M-C) simulations of the proposed Heisenberg model, taking the spins as classical three-component vectors with the constraint that the modulus is fixed to 1. We used the standard Metropolis algorithm combined with over relaxation (micro canonical) updates. One hybrid M-C step (M-CS) consists of one canonical MC step

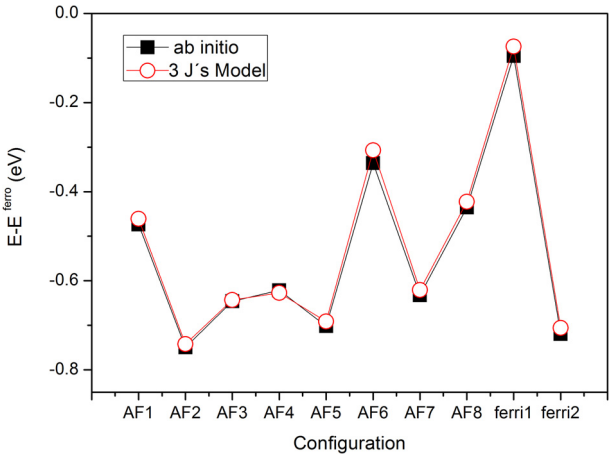

Figure 3. Energy of each magnetic configuration, referred to the ferromagnetic case obtained in the ab-initio calculations (open black squares) and that obtained in the framework of the Heisenberg model (full red circles). For details of the configurations, see Table 2.

Table 2. Spin configurations used for the determination of the coupling constants J^i_{BB} ($i = 1, 2, 3, 4, 5$). $\pm$ indicates the relative spin orientations in the $\{a \times a \times 2a\}$ super-cell (112 atoms).

Fe atom at	FM	AF1	AF2	AF3	AF4	AF5	AF6	AF7	AF8	FERRI1	FERRI2
0.5; 0.5; 0.25	+	+	+	−	−	+	+	+	+	−	+
0.5; 0.5; 0.75	+	+	+	−	−	+	−	−	+	+	+
0.5; 0.25; 0.125	+	+	+	+	−	+	+	−	+	+	−
0.5; 0.25; 0.625	+	+	+	+	−	+	−	+	−	+	−
0.0; 0.0; 0.25	+	+	+	+	+	+	+	+	+	+	+
0.0; 0.0; 0.75	+	+	+	+	+	+	−	−	+	+	+
0.0; 0.75; 0.125	+	+	+	−	−	−	+	−	+	+	−
0.0; 0.75; 0.625	+	+	+	−	−	−	−	+	−	+	+
0.0; 0.5; 0.0	+	+	−	−	+	−	+	−	+	+	−
0.0; 0.5; 0.5	+	+	−	−	+	−	−	+	−	+	−
0.0; 0.25; 0.375	+	+	−	+	+	+	+	+	−	+	+
0.0; 0.25; 0.875	+	+	−	+	+	+	−	−	−	+	+
0.5; 0.0; 0.0	+	+	−	−	−	−	+	+	+	+	+
0.5; 0.0; 0.5	+	+	−	−	−	−	−	−	−	+	−
0.5; 0.75; 0.375	+	+	−	−	−	−	+	+	−	+	+
0.5; 0.75; 0.875	+	+	−	−	−	−	−	−	−	+	+
0.75; 0.75; 0.25	+	−	−	+	+	+	+	−	+	+	−
0.75; 0.75; 0.75	+	−	−	+	+	+	−	+	+	+	−
0.25; 0.5; 0.125	+	−	−	+	+	+	+	+	+	+	+
0.25; 0.5; 0.625	+	−	−	+	+	+	−	−	−	+	+
0.25; 0.25; 0.25	+	−	−	−	−	−	+	−	+	+	−
0.25; 0.25; 0.75	+	−	−	−	−	−	−	+	+	+	−
0.75; 0.0; 0.125	+	−	−	+	+	−	+	+	+	+	+
0.75; 0.0; 0.625	+	−	−	+	+	−	−	−	−	+	+
0.25; 0.75; 0.0	+	−	+	−	−	+	+	+	+	+	+
0.25; 0.75; 0.5	+	−	+	−	−	+	−	−	−	+	+
0.75; 0.5; 0.375	+	−	+	+	+	−	+	−	−	+	−
0.75; 0.5; 0.875	+	−	+	+	+	−	−	+	−	+	−
0.75; 0.25; 0.0	+	−	+	+	+	+	+	−	+	+	+
0.75; 0.25; 0.5	+	−	+	+	+	+	−	+	−	+	+
0.25; 0.0; 0.375	+	−	+	−	−	−	+	−	−	+	−
0.25; 0.0; 0.875	+	−	+	−	−	−	−	+	−	+	−

https://doi.org/10.1016/j.heliyon.2019.e01170

followed by $3-10$ micro canonical random updates [25, 26] depending on cluster size. The classical M-C simulations were performed on periodic lattices of $N = 16 \times L^3$ spins with linear sizes $L = 2-8$. For each magnetic field or temperature we discarded 1×10^5 hybrid Monte-Carlo steps (MCS) for initial relaxation and data were collected during subsequent 2×10^5 MCS.

Our main goal is to compare the experimental and simulation results on the thermal dependence of the magnetic susceptibility of normal $ZnFe_2O_4$. To this end, we expect firstly to reproduce the main features of its macroscopic magnetic behavior, such as the ordering temperature T_N and the C-W behavior of the susceptibility at temperatures higher than T_N. Therefore, we calculated the specific heat C_v and χ in the temperature range 1-300 K as:

$$C_v = \frac{\langle E^2 \rangle - \langle E \rangle^2}{NT^2} \qquad \chi = \frac{1}{3NT} \sum_{a=x,y,z} \langle (M^a)^2 \rangle - \langle M^a \rangle^2 \tag{2}$$

where $E = \langle H \rangle$ is the energy of the system, $M^a = \sum_i S_i^a$ is the total magnetization, $a = x, y, z$ and $\langle\rangle$ stands for the ensemble average [27].

The M-C simulation results are shown in Figure 4. We observe that the C_v behavior is consistent with a first-order phase transition that takes place at $\sim$ 11 K, in accordance with the experimental reports ([28, 29]). On the other hand, the $\chi(T)$ curve has a cusp-like peak at around 13 K. In addition, above this temperature χ^{-1} shows a linear dependence while the asymptotic C-W behavior gives rise to a large and negative $\Theta_{CW} = -170_1$ K (Figure 4, left). Therefore, the M-C simulations performed using a Heisenberg model with exchange couplings obtained from ab-initio calculations reproduces quite well both the transition temperature and the cusp-like feature in $\chi(T)$ usually reported for $ZnFe_2O_4$ [3]. On the other hand, while the analysis of all experimental results accounts for a departure from a C-W behavior from high temperatures, which involves a high and positive Θ_{CW}, the simulation predicts that the C-W law holds above T_N resulting in a negative Θ_{CW}. In any case, the $|\Theta_{CW}|/T_N$ ratio higher than 10 classifies normal $ZnFe_2O_4$ as a strongly geometrically frustrated magnetic compound [10].

3. Discussion

In order to discuss a possible origin of the discrepancy between experimental data and the above simulations results, in the following we will perform a careful inspection of experimental DC susceptibility curves ($\chi = M/H$, $\mu_0 H = 50$ mT) of $ZnFe_2O_4$ polycrystalline samples (ZFO and ZFO-370) reported in ref. [30]. The ZFO sample was prepared by solid state reaction from its precursors oxides. This sample presents a slight inversion, which was detected from its Fe L_3-edge x-ray magnetic circular dichroism (XMCD) spectrum [30]. Treatments under vacuum at

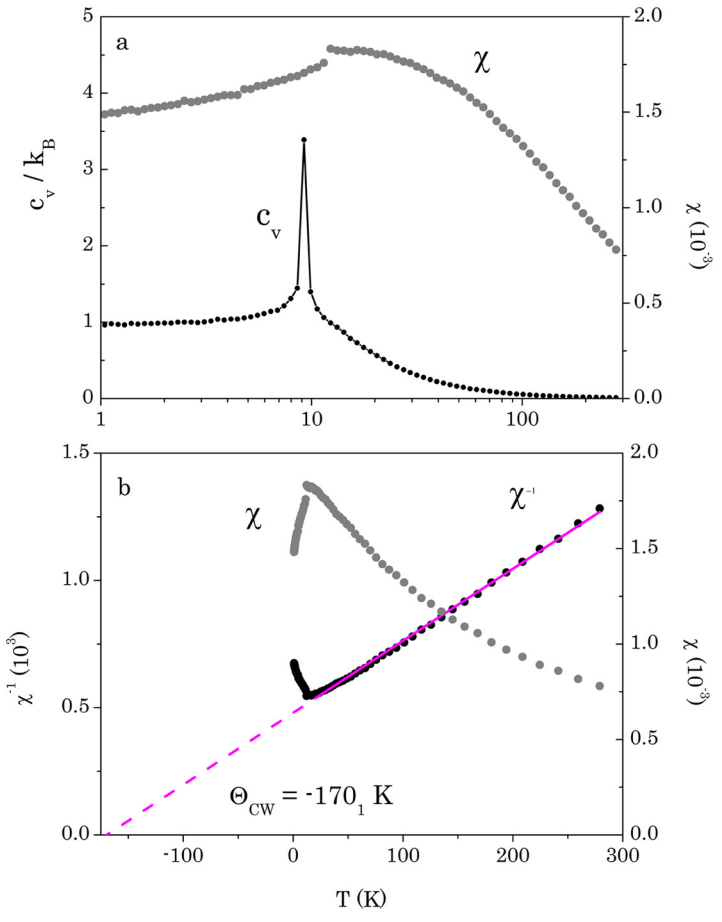

Figure 4. (a) Susceptibility χ and specific heat C_v as a function of temperature plotted on a logarithmic scale. (b) χ and χ^{-1} as a function of temperature obtained from Monte-Carlo simulations. The solid line corresponds to the linear fit of the high temperature values of χ^{-1}. The dashed line shows the extrapolation of the fit to obtain Θ_{CW}.

moderate temperatures (up to 450 °C) diminish the cation inversion preserving the spinel structure. The inversion level of sample annealed at 370 °C (ZFO-370) is below the XMCD detection limit [30], i.e. the magnetic cations are mainly at *B*-sites.

For both samples, the thermal dependence of χ presents similarities such as a cusp around 13 K as well as a broad bump within the 40 to 80 K range (Figure 5 (a)). We observe that χ^{-1} (Figure 5 (b)) presents similar features to those previously reported for $ZnFe_2O_4$ (see, for instance, Ref. [3]). Indeed, a deviation from a C-W behavior can be appreciated below 200 K, while the Θ_{CW} temperatures obtained by extrapolation from temperatures above the linear region of χ^{-1} are positive and relatively high ($+169_1$ K and $+117_1$ K for ZFO and ZFO-370, respectively). A higher inversion in $ZnFe_2O_4$ not only increases the magnetization values but also enhances the convex shape of χ above the transition temperature [3], i.e. it affects the magnetic response in a range of temperatures $T_N < T < |\Theta_{CW}|$. Considering that

https://doi.org/10.1016/j.heliyon.2019.e01170

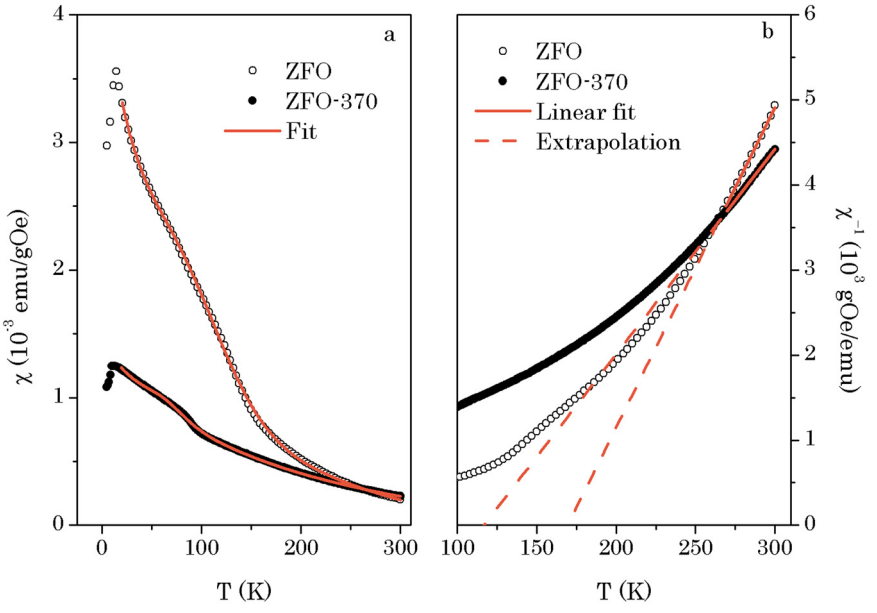

Figure 5. (a) DC susceptibilities of samples ZFO and ZFO-370. The solid lines are the result from the fitting using eq. (3). (b) Reciprocal susceptibility χ^{-1}. Solid lines represent the linear fit in the high-temperature range, the dashed lines show the extrapolations of the high-temperature C-W behavior.

Table 3. Parameters obtained by fitting Eq. (3) to the experimental susceptibility in the 20 to 300 K temperature range.

Sample	χ_{dia} (10^{-4} emu/g Oe)	A (10^{-4} emu.g^{-1}.Oe^{-1})	T_b (K)	σ (K)	C (emu.K.g^{-1}.Oe^{-1})	Θ_{CW} (K)
ZFO	-5.5_3	7.3_3	76_1	45_1	0.26_1	-54_2
ZFO-370	-4.3_8	0.80_2	57_1	19.5_8	0.305_5	-164_3

a slight inversion is frequently detected in bulk normal $ZnFe_2O_4$ [3], the broad peak observed in χ at intermediate temperatures above T_N could account for the blocking of moments of ferro- or ferrimagnetic sample regions. Assuming this hypothesis, the χ experimental data between 20 and 300 K were fitted using the following expression:

$$\chi = \frac{C}{T + \Theta_{CW}} + A \exp^{-\frac{(T-T_b)^2}{2\sigma}} + \chi_{\text{dia}} \tag{3}$$

where the first term represents the intrinsic C-W contribution (where C is the Curie constant), the second one is a Gaussian function of amplitude A and width σ considered to account for the broad peak centered at a temperature T_b and χ_{dia} is a diamagnetic contribution. The fitting results are shown in Table 3 and Figure 5(a). We observe that the χ data above T_N of ZFO and ZFO-370 are quite well reproduced by the proposed function (see Figure 5(a)). It is worth noticing that the fitting parameter Θ_{CW} reaches a negative value and, moreover, for the sample with a negligible inversion (ZFO-370) Θ_{CW} agrees well with that one obtained from M-C simulations.

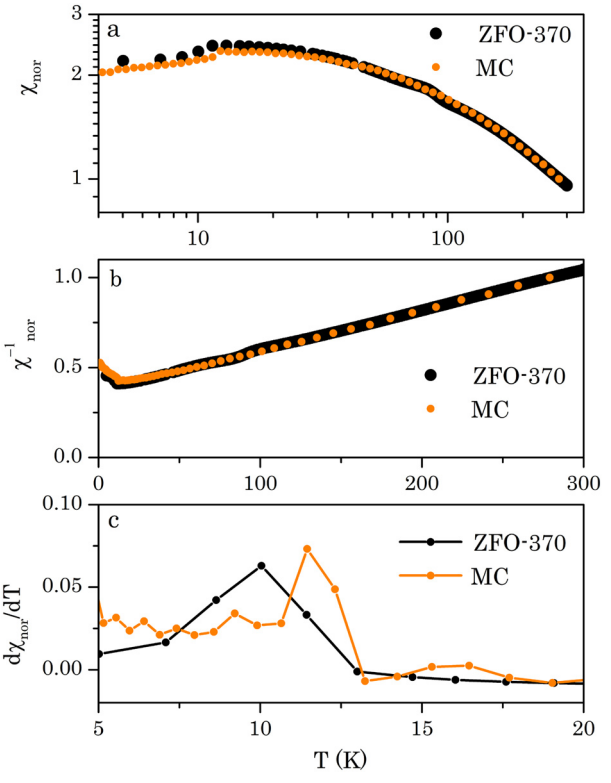

Figure 6. Comparison of experimental data after the substraction of gaussian and diamagnetic contributions and M-C results, (a) χ, (b) χ^{-1} and (c) $d\chi/dT$.

The χ of ZFO-370 that results after subtracting the Gaussian and diamagnetic components are presented in Figure 6(a), in addition with the simulation results. For comparison, these curves were normalized to their values at $T = 290$ K (χ_{nor}). In addition, the reciprocal $\chi^{-1}_{\rm nor}$ and $\chi_{\rm nor}$ derivative are presented in Figures 6 (b) and (c), respectively. The good agreement between experimental and simulated results suggest that the proposed model reproduces the intrinsic C-W contribution extracted from the experimental data

Motivated by the results given above, we inspect the magnetic configuration of $ZnFe_2O_4$ predicted by our model. We found that the module of total spin per tetrahedron is zero, and furthermore, the spins cancel out in pairs. To show this, in Figure 7 we plot at $L = 6, 8$ all the average scalar products between pairs of the four spins per tetrahedron, averaged over all the lattice, as a function of temperature. It can be clearly seen that two pairs are antiparallel, and that all the other scalar products average out to zero. These results are for one realization of the simulations, since the opposite-spin pairs will change in each realization (for example, in Figure 7 for $L = 6$ these pairs are for spins $1-3, 2-4$ and for $L = 8$ they are $1-4, 2-3$).

The arrangement between tetrahedra is a somewhat more cumbersome matter. Inspecting the magnetic structure at the lowest simulated temperatures, we find an

 https://doi.org/10.1016/j.heliyon.2019.e01170

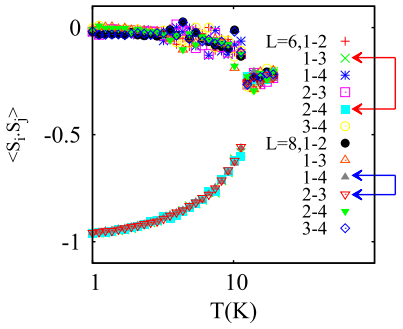

Figure 7. $\langle \vec{S}_i \vec{S}_j \rangle$ calculated for the four spins (1,2,3,4) in each tetrahedron, for one realization at $L = 6$ and one at $L = 8$. The arrows indicate the antiparallel spin pairs.

incommensurate spiral order in two of the three cartesian directions, with an order vector $\vec{q}$ that depends on system size. A detailed characterization of the interplay between these antiferromagnetic couplings and the effect in the low temperature magnetic states is deferred for future work.

4. Conclusions

In this work, we present a combined ab-initio and Monte-Carlo study of the magnetic properties of normal $ZnFe_2O_4$. We focused mainly on the magnetic susceptibility, comparing experimental data with Monte-Carlo simulations assuming a classical Heisenberg spin model with exchange constants obtained by ab-initio calculations.

Firstly, assuming spinel structure with a normal distribution of cations (where the magnetic moments at octahedral sites form a pyroclore lattice), we calculated exchange couplings up to fifth-nearest neighbors using ab initio DFT calculations. We found that all the interactions are antiferromagnetic. In particular, the third-nearest neighbor interaction was comparable to the first-nearest neighbor one, and thus relevant to determine the low-temperature magnetic configuration. The fourth and fifth-nearest neighbors interactions are negligible.

Secondly, the obtained couplings were used in Monte-Carlo Metropolis simulations to reproduce the magnetic susceptibility of normal $ZnFe_2O_4$. The simulation results considering such a simple model and assuming interactions up to third-neighbors, predict a Curie–Weiss behavior at high temperatures and, contrary to previous reports, to a negative Θ_{CW}. A very good agreement with the experimental data could be achieved after extracting spurious contributions mainly coming from inverted sample regions. Specifically, the T_N (13 K) and Θ_{CW} (−170 K) values match quite well with the experimental data considering only the intrinsic contributions. We conclude that the susceptibility of pure normal $ZnFe_2O_4$ presents features compatible with other isomorphic spinels with strong geometrical frustration due to unsatisfied AFM interactions between magnetic ions at the pyrochlore *B*-sublattice.

 https://doi.org/10.1016/j.heliyon.2019.e01170

As for the magnetic order below the T_N, Monte-Carlo results show that for $T < T_N$ there is a local order per tetrahedron, where the four spins are arranged in antiparallel pairs.

Declarations

Author contribution statement

J. Melo Quintero, K.L. Salcedo Rodríguez, H.D. Rosales: Performed the experiments; Analyzed and interpreted the data.

F.A. Gómez Albarracín: Performed the experiments; Analyzed and interpreted the data; Contributed reagents, materials, analysis tools or data.

P. Mendoza Zélis: Analyzed and interpreted the data.

S.J. Stewart: Analyzed and interpreted the data; Wrote the paper.

L.A. Errico: Performed the experiments; Analyzed and interpreted the data; Contributed reagents, materials, analysis tools or data; Wrote the paper.

C. Rodríguez Torres: Conceived and designed the experiments; Analyzed and interpreted the data; Contributed reagents, materials, analysis tools or data; Wrote the paper.

Funding statement

This work was supported by CONICET (PIP0813, PIP0720, PIP0046), UNLP (11/X678, 11/X680, 11/X708, 11/X788, 11/X792), ANPCyT (PICT 2012-1724, 2013-2616, 2016-4083) and UNNOBA (SIB2017).

Competing interest statement

The authors declare no conflict of interest.

Additional information

No additional information is available for this paper.

 https://doi.org/10.1016/j.heliyon.2019.e01170

References

[1] K. Kamazawa, Y. Tsunoda, H. Kadowaki, K. Kohn, Magnetic neutron scattering measurements on a single crystal of frustrated $ZnFe_2O_4$, Phys. Rev. B 68 (2003) 024412, https://doi.org/10.1103/PhysRevB.68.024412.

[2] H. Mamiya, N. Tsujii, N. Terada, S. Nimori, H. Kitazawa, A. Hoshikawa, T. Ishigaki, Slow dynamics in the geometrically frustrated magnet $ZnFe_2O_4$: universal features of aging phenomena in spin glasses, Phys. Rev. B 90 (2014) 014440, https://doi.org/10.1103/PhysRevB.90.014440.

[3] T. Usa, K. Kamazawa, H. Sekiya, S. Nakamura, Y. Tsunoda, K. Kohn, M. Tanaka, Magnetic properties of $ZnFe_2O_4$ as a 3-D geometrical spin frustration system, J. Phys. Soc. Jpn. 73 (2004) 2384, https://doi.org/10.1143/JPSJ.73.2834.

[4] W. Schiessl, W. Potzel, H. Karzel, M. Steiner, G.M. Kalvius, A. Martin, M.K. Krause, I. Halevy, J. Gal, W. Schafer, G. Will, M. Hillberg, E. Wappling, Magnetic properties of the $ZnFe_2O_4$ spinel, Phys. Rev. B 53 (1996) 9143, https://doi.org/10.1103/PhysRevB.53.9143.

[5] T. Watanabe, S. Tadataka, K. Tomiyasu, K. Kamazawa, Acoustic study of dynamical molecular-spin state without magnetic phase transition in spin-frustrated $ZnFe_2O_4$, Phys. Rev. B 92 (2015) 174420, https://doi.org/10.1103/PhysRevB.92.174420.

[6] D.J. Singh, M. Gupta, R. Gupta, Density-functional description of spinel $ZnFe_2O_4$, Phys. Rev. B 63 (2001) 205102, https://doi.org/10.1103/PhysRevB.63.205102.

[7] K. Tomiyazu, K. Kamazawa, A spin molecule model for geometrically frustrated spinel $ZnFe_2O_4$, J. Phys. Soc. Jpn. 80 (2011) SB024, https://doi.org/10.1143/JPSJS.80SB.SB024.

[8] S.T. Bramwell, M.J.P. Gingras, P.C.W. Holdsworth, Spin ice, in: Frustrated Spin Systems: 2nd, World Scientific, 2013, pp. 383–474.

[9] J.E. Greedan, Geometrically frustrated magnetic materials, J. Mater. Chem. 11 (2001) 37, https://doi.org/10.1039/B003682J.

[10] A.P. Ramirez, Strongly geometrically frustrated magnets, Annu. Rev. Mater. Sci. 24 (1994) 453, https://doi.org/10.1146/annurev.ms.24.080194.002321.

[11] S.H. Lee, H. Takagi, D. Louca, M. Matsuda, S. Ji, H. Ueda, Y. Ueda, T. Katsufuji, J. Chung, S. Park, S. Cheong, C. Broholm, Frustrated magnetism and cooperative phase transitions in spinels, J. Phys. Soc. Jpn. 79 (2010) 011004, https://doi.org/10.1143/JPSJ.79.011004.

[12] M.A. Hakim, M. Manjurul Haque, M. Huq, P. Nordblad, Spin-glass-like ordering in the spinel $ZnFe_2O_4$ ferrite, Physica B 406 (2011) 48, https://doi.org/10.1016/j.physb.2010.10.010.

[13] K. Kamazawa, S. Park, S.H. Lee, T.J. Sato, Y. Tsunoda, Dissociation of spin objects in geometrically frustrated $CdFe_2O_4$, Phys. Rev. B 70 (2004) 024418, https://doi.org/10.1103/PhysRevB.70.024418.

[14] A.J. Garcia-Adeva, D.L. Huber, Quantum tetrahedral mean field theory of the magnetic susceptibility for the pyrochlore lattice, Phys. Rev. Lett. 85 (2000) 4598, https://doi.org/10.1103/PhysRevLett.85.4598.

[15] Y. Yamada, K. Kamazawa, Y. Tsunoda, Interspin interactions in $ZnFe_2O_4$: theoretical analysis of neutron scattering study, Phys. Rev. B 66 (2002) 064401, https://doi.org/10.1103/PhysRevB.66.064401.

[16] P.H. Conlon, J.T. Chalker, Absent pinch points and emergent clusters: further neighbor interactions in the pyrochlore Heisenberg antiferromagnet, Phys. Rev. B 81 (2010) 224413, https://doi.org/10.1103/PhysRevB.81.224413.

[17] A.N. Yaresko, Electronic band structure and exchange coupling constants in ACr_2X_4 spinels (A=Zn, Cd, Hg; X=O, S, Se), Phys. Rev. B 77 (2008) 115106, https://doi.org/10.1103/PhysRevB.77.115106.

[18] Ching Cheng, Long-range antiferromagnetic interactions in $ZnFe_2O_4$ and $CdFe_2O_4$: density functional theory calculations, Phys. Rev. B 78 (2008) 132403, https://doi.org/10.1103/PhysRevB.78.132403.

[19] P. Blaha, K. Schwarz, G. Madsen, D. Kvasnicka, J. Luitz, WIEN2k, an Augmented Plane Wave Plus Local Orbitals Program for Calculating Crystal Properties, Technical Universität Wien, Austria, 1999.

[20] E. Sjostedt, L. Nordstrom, D.J. Singh, An alternative way of linearizing the augmented plane-wave method, Solid State Commun. 114 (2000) 15, https://doi.org/10.1016/S0038-1098(99)00577-3.

[21] S. Cottenier, Density Functional Theory and the Family of (L)APW-methods: a Step-by-Step Introduction, KU Leuven, Belgium, 2002.

[22] Z. Wu, R.E. Cohen, More accurate generalized gradient approximation for solids, Phys. Rev. B 73 (2006) 235116, https://doi.org/10.1103/PhysRevB.73.235116.

[23] V.I. Anisimov, J. Zaanen, O.K. Andersen, Band theory and Mott insulators: Hubbard U instead of Stoner I, Phys. Rev. B 44 (1991) 943, https://doi.org/10.1103/PhysRevB.44.943.

[24] J.J. Melo Quintero, C.E. Rodríguez Torres, L.A. Errico, Ab initio calculation of structural, electronic and magnetic properties and hyperfine parameters at the Fe sites of pristine $ZnFe_2O_4$, J. Alloys Compd. 741 (2018) 746, https://doi.org/10.1016/j.jallcom.2018.01.217.

[25] F.R. Brown, T.J. Woch, Overrelaxed heat-bath and Metropolis algorithms for accelerating pure gauge Monte Carlo calculations, Phys. Rev. Lett. 58 (1987) 2394, https://doi.org/10.1103/PhysRevLett.58.2394.

[26] M. Creutz, Overrelaxation and Monte Carlo simulation, Phys. Rev. D 36 (1987) 515, https://doi.org/10.1103/PhysRevD.36.515.

[27] M.E.J. Newman, G.T. Barkema, Monte Carlo Methods in Statistical Physics, Oxford University Press, New York, 2001.

[28] E.F. Westrum Jr., D.M. Grimes, Low-temperature heat capacities and thermodynamic properties of zinc ferrites—III: effect of copper substitution, J. Phys. Chem. Solids 10 (1959) 120, https://doi.org/10.1016/0022-3697(59)90065-4.

[29] J.C. Ho, H.H. Hamdeh, Y.Y. Chen, S.H. Lin, Y.D. Yao, R.J. Willey, S.A. Oliver, Low-temperature calorimetric properties of zinc ferrite nanoparticles, Phys. Rev. B 52 (1995) 10122, https://doi.org/10.1103/PhysRevB.52.10122.

[30] K. Salcedo Rodríguez, S.J. Stewart, P. Mendoza Zélis, G. Pasquevich, C.E. Rodríguez Torres, Role of defects on the magnetic behaviour of the geometrically frustrated spinel $ZnFe_2O_4$, J. Alloys Compd. 752 (2018) 289, https://doi.org/10.1016/j.jallcom.2018.04.172.